Bimetallic Au/Ag Core–Shell Nanorods Studied by Ultrafast Transient Absorption Spectroscopy under Selective Excitation

ARTICLE *in* THE JOURNAL OF PHYSICAL CHEMISTRY C · JUNE 2011

Impact Factor: 4.77 · DOI: 10.1021/jp201648v

4 AUTHORS:

Kuai Yu
Stanford University
20 PUBLICATIONS **547** CITATIONS
SEE PROFILE

Guanjun You
Pennsylvania State University
44 PUBLICATIONS **555** CITATIONS
SEE PROFILE

Polavarapu Lakshminarayana
Ludwig-Maximilians-University of Munich
44 PUBLICATIONS **1,273** CITATIONS
SEE PROFILE

Qing-Hua Xu
National University of Singapore
129 PUBLICATIONS **3,337** CITATIONS
SEE PROFILE

THE JOURNAL OF PHYSICAL CHEMISTRY C

ARTICLE

pubs.acs.org/JPCC

Bimetallic Au/Ag Core–Shell Nanorods Studied by Ultrafast Transient Absorption Spectroscopy under Selective Excitation

Kuai Yu,[†,‡] Guanjun You,[†] Lakshminarayana Polavarapu,[†] and Qing-Hua Xu[*,†,‡]

[†]Department of Chemistry, National University of Singapore, Singapore 117543

[‡]NUS Graduate School for Integrative Sciences and Engineering, National University of Singapore, Singapore, 117456

ABSTRACT: Au/Ag core–shell nanorods with variable shell thickness were prepared by using a simple method, and their optical properties were characterized by using steady state extinction spectra and ultrafast transient absorption spectroscopy. The extinction spectra and discrete dipole approximation calculations showed that the longitudinal surface plasmon resonance (SPR) peak of Au/Ag core–shell nanorods shifted to blue as the Ag shell thickness increased. Although these Au/Ag core–shell nanorods are expected to display two longitudinal SPR bands, only one longitudinal SPR band was observed in the steady state extinction spectra and simulation results. We resolved this conflict by using ultrafast transient absorption spectroscopy under different excitation wavelengths: 400 and 800 nm. We have experimentally demonstrated for the first time the existence of two closely spaced longitudinal SPR bands in Au/Ag core–shell nanorods, corresponding to the contributions from the Ag shell and Au core.

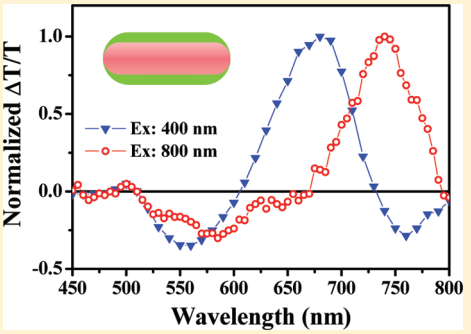

INTRODUCTION

Noble metal nanoparticles such as Au and Ag have been the subject of intensive research due to their unique optical properties and various potential applications in biosensing,[1−3] imaging,[4−7] photothermal cancer therapy,[8] and optical data storage.[9,10] Au and Ag nanorods (NRs) are of particular interest due to their tunable surface plasmon resonance (SPR) from visible to near IR, which is highly dependent on their aspect ratios and local surrounding media.[11] Compared to pure Au and Ag NRs, bimetallic compound nanomaterials display superior optical properties and have been less studied. Pastoriza-Santos et al.[12] reported that the optical properties of thin Ag shell coated Au NRs are similar to those of pure Ag NRs rather than pure Au NRs. Even a thin Ag shell has a strong influence on the surface plasmons of the Au/Ag core–shell structure.

In addition to UV–visible extinction spectroscopy, many computational methods such as discrete dipole approximation (DDA),[11,13−15] the boundary element method (BEM),[16] and finite difference in the time domain method (FDTD)[17] have also been used to characterize the optical properties of noble metal nanoparticles. These simulation results are usually in good agreement with the experimental observations. Ma et al.[18] experimentally observed two SPR bands at 410 and 510 nm in Au/Ag core–shell nanocubes, which are characteristics of the Ag shell and Au core, respectively. In a simulation of SPR spectra of Au/Ag core–shell nanowires, Zhu[19] has theoretically demonstrated two transverse SPR bands at 410 and 530 nm. One was ascribed to the outer Ag shell, which is similar to the SPR response of pure Ag nanoparticles. The other band was ascribed to the contribution from the interface between the core and shell of the core–shell nanowires, which is similar to the Au nanoparticles. Since two transverse SPR bands have been observed in Au/Ag core–shell nanoparticles, it is expected that two longitudinal SPRs should exist in Au/Ag core–shell NRs. However, only one longitudinal mode has been observed.[12,13,20−22] The inconsistence indicates that the steady state extinction spectra could not distinguish two longitudinal SPR bands in Au/Ag core–shell NRs.

Recently, ultrafast transient absorption and pump probe spectroscopy have been used as a novel and powerful tool to characterize the optical properties of noble metal nanoparticles.[23−26] In a transient absorption experiment, a pump beam promotes the electrons to an elevated temperature, and a time-delayed probe beam monitors the induced changes and subsequent dynamics. Most of the previous transient absorption studies were conducted on monometallic nanoparticles.[24,27−30] To the best of our knowledge, there are no transient absorption studies on bimetallic Au/Ag core–shell NRs. If different plasmon bands in Au/Ag core–shell NRs can be selectively excited, it is possible to selectively detect the plasmon bands arising from the Ag shell and Au core. To experimentally prove this concept and demonstrate the existence of two longitudinal SPRs in Au/Ag core–shell NRs, we have conducted transient absorption measurements on these materials under two different excitation wavelengths: 400 and 800 nm. We have prepared uniformly coated Au/Ag core–shell NRs with variable shell thickness by a rapid reduction method using $NaBH_4$ as the reducing agent. The optical properties of the prepared Au/Ag core–shell NRs were characterized by using steady state extinction spectra and transient absorption measurements. Consistent with the previous

Received: February 19, 2011
Revised: May 26, 2011

   dx.doi.org/10.1021/jp201648v | *J. Phys. Chem. C* XXXX, XXX, 000–000

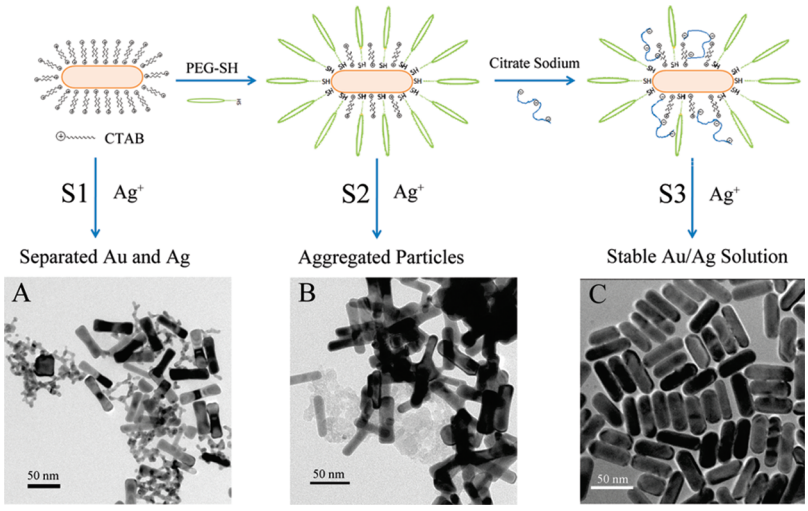

Figure 1. Schematic representation of the preparation processes of Au/Ag core−shell NRs using three different surfactant-coated Au NRs as seeds (S1, S2, and S3): S1, CTAB-coated Au NRs; S2, PEGylated Au NRs; S3, citrate ion stabilized PEGylated Au NRs. The corresponding TEM images of the synthesized Au/Ag bimetallic nanoparticles are also shown.

studies, only one longitudinal SPR band was observed from the steady state extinction spectra and the simulation results.[13,20] However, our transient absorption studies demonstrate the existence of two longitudinal SPR bands in Au/Ag core−shell NRs that are due to the contributions from the Ag shell and the Au core.

EXPERIMENTAL SECTION

Chemicals. Hydrogen tetrachloroaurate (III) trihydrate ($HAuCl_4 \cdot 3H_2O$), silver nitrate ($AgNO_3$), sodium citrate, sodium borohydride ($NaBH_4$), L-ascorbic acid, polyethylene glycol thiol (PEG-SH), cetyltrimethylammonium bromide (CTAB), and hydrochloric acid (HCl) were purchased from Sigma-Aldrich. All chemical reagents were used without further purification. Water used in the preparation of all samples was purified with cartridges from Millipore (Nanopure, Barnstead, USA) to a resistivity of >18.0 MΩ cm.

Preparation of Au/Ag Core−Shell NRs. Au NRs with a longitudinal SPR band maximum at 820 nm were first synthesized by using a previously reported seed-mediated growth method.[31,32] The seed solution was prepared by adding 25 μL of 0.1 M $HAuCl_4$ to 10 mL of 0.1 M CTAB solution in a plastic tube. A freshly prepared 0.6 mL of ice-cold 0.01 M $NaBH_4$ solution was quickly added all at once under vigorous stirring. The stirring continued for another 2 min, and the resulting brownish yellow solution was kept at room temperature for at least 2 h to be used as the seed solution. For seed-mediated growth, 2.0 mL of 0.01 M $HAuCl_4$ and 0.4 mL of 0.01 M $AgNO_3$ were added into 40 mL of 0.1 M CTAB solution and mixed by gentle shaking. Freshly prepared 0.32 mL of 0.1 M L-ascorbic acid solution and 0.8 mL of 1.0 M HCl were then added sequentially. Seed solution (100 μL) was added into the reaction mixture and then left undisturbed overnight for longitudinal overgrowth. The prepared Au NRs were purified by centrifugation of NR solution with a speed of 12 000 rpm for 10 min to remove excess CTAB surfactant twice. The resulting Au NRs were used for the subsequent preparation of Au/Ag core−shell NRs.

Au/Ag core−shell NRs were successfully prepared by reducing the silver ions in the presence of PEG-SH capped Au NRs and sodium citrate. First, PEG-SH capped Au NRs were prepared by using a method previously reported by Thierry et al.[33] Briefly, the purified Au NRs (5 mL) were mixed with 2 mL of 1.28 mM PEG-SH, and the reaction was left overnight under vigorous stirring. Excess PEG molecules were removed by centrifugation at 7000 rpm for 10 min, and the PEGylated Au NRs were re-dispersed in 5 mL of water. Three parallel processes were tried to screen the best reaction conditions for the preparation of Au/Ag core−shell NRs by using three types of surface-modified Au NRs as seed solutions: (1) 5 mL of CTAB-coated Au NRs, (2) 5 mL of PEGylated Au NRs, and (3) 5 mL of PEGylated Au NRs with 1 mL of 0.2 M citrate sodium solution added as a stabilizing agent. A certain amount of 1 mM $AgNO_3$ and 0.1 M $NaBH_4$ were added into different seed solutions sequentially. The reaction mixture was left for several minutes under vigorous stirring. Finally, the synthesized Au/Ag core−shell NRs were purified by centrifugation at 6000 rpm twice for 10 min and then dispersed in the same amount of water.

Characterizations. The UV−visible extinction spectra of the samples were measured by using a Shimadzu UV 2450 spectrometer. Transmission electron micrograph (TEM) images were taken by using a JEOL 2010 electron microscope. The transient absorption experiments were performed by using a Spectra Physics Ti:sapphire oscillator seeded amplifier laser system. The 800 nm output of the amplifier laser system has a pulse energy of 2 mJ with a repetition rate of 1 kHz. The 800 nm laser beam was split into two portions. The larger portion was used directly as the pump beam (for 800 nm excitation) or passed through a BBO crystal to generate 400 nm pulses by second harmonic generation to act as the pump beam (for 400 nm excitation). The small portion of the 800 nm beam was focused onto a 1 mm sapphire plate to generate a white light continuum. The white light beam was split into two portions: one as the probe and another as the reference to correct the pulse-to-pulse intensity fluctuations. The pump beam was focused on the sample with a beam size of 300 μm and overlapped with the smaller probe beam (100 μm in diameter). The time delay between the pump and probe pulses was varied by using a computer-controlled translation stage (Newport, ESP 300). All the transient absorption experiments were performed at room

dx.doi.org/10.1021/jp201648v |J. Phys. Chem. C XXXX, XXX, 000–000

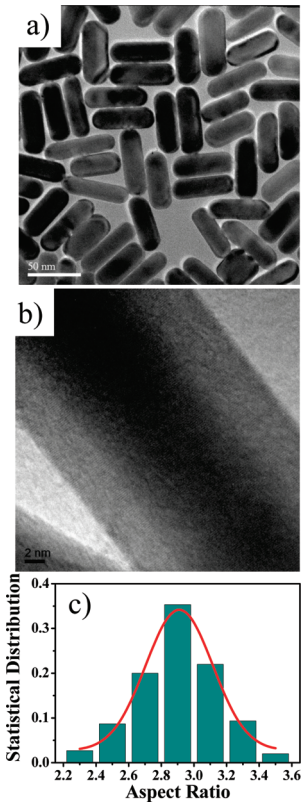

Figure 2. (a) Typical TEM image of the prepared Au/Ag core−shell NRs with a longitudinal SPR band centered at 690 nm and (b) a high-resolution TEM image of Au/Ag core−shell NRs. The average thickness of the silver shell is around 4 nm. (c) Histogram of the aspect ratio distribution and the corresponding Gaussian fit of the obtained Au/Ag core−shell NRs. The statistical analysis of the aspect ratio was evaluated from TEM images of more than 200 nanoparticles.

temperature with the aqueous nanoparticles contained in a 1 mm path length cuvette. During the measurements, the pump and probe pulse energies were kept low to minimize the photodamage to the samples.

RESULTS AND DISCUSSIONS

Three different methods were used to prepare Au/Ag core−shell NRs (Figure 1). In the first approach, CTAB-coated Au NRs were used as the seeds (S1) to prepare Au/Ag core−shell NRs. Only a mixture of pure Ag nanoparticles and Au NRs were obtained (Figure 1A). No Ag was coated on the Au NRs. The rapidly reduced Ag atoms self-nucleated to form Ag nanoparticles. This is due to densely absorbed CTAB double layers on the Au NRs, which inhibit epitaxial growth of Ag on the Au surfaces.[34] To reduce the inhibition from the CTAB surfactant on the Au NR surface, the ligand exchange method was used to replace CTAB with PEG-SH molecules. PEG-SH was known able to replace CTAB from the surface of gold NRs and reduce the density of CTAB.[33] UV−visible extinction spectra were used to characterize the ligand exchange process. The longitudinal SPR band of Au NRs was observed to blue-shift for 10 nm after the ligand exchange. In the second approach, PEGylated Au NRs were used as the seeds (S2) for the Ag coating. After adding the reducing agent-$NaBH_4$, the particles were found to precipitate at the bottom of the container. The TEM image showed that the Au NRs were partially coated but coalesced together (Figure 1B).

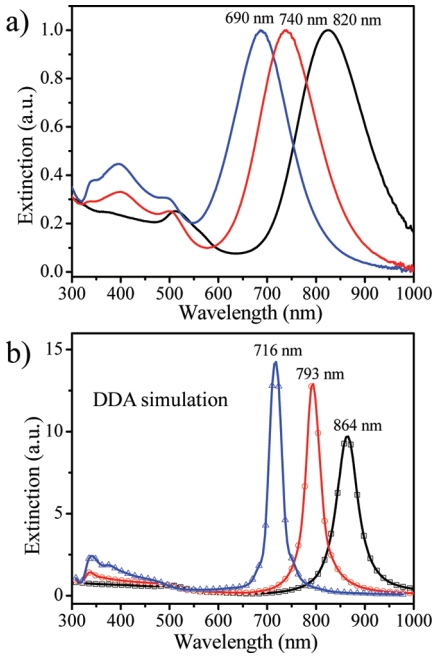

Figure 3. (a) UV−visible extinction spectra of Au NRs and Au/Ag core−shell NRs with different thicknesses of Ag coating and (b) the corresponding calculated extinction spectra of pure Au NRs and Au/Ag core−shell NRs by DDA simulations.

The nanoparticle solutions prepared by this method were unstable. Citrate ions were known able to stabilize the Ag nanoparticles.[35] When sodium citrate stabilized PEGylated Au NRs were used as the seeds (S3), well-separated, stable Au/Ag core−shell NRs were finally prepared successfully (Figure 1C).

Figure 2 shows the typical TEM images of Au/Ag core−shell NRs prepared by using method 3, with a longitudinal SPR band centered at 690 nm. The Au NRs were uniformly coated with Ag. The boundary between Ag and Au can be easily distinguished by the brightness contrast. Ag was found to grow preferentially on the lateral facets of the Au NRs. The preferential growth might be due to the PEG-SH binding to the ends of Au NRs, which completely blocks the longitudinal growth of Au NRs.[12] The high-resolution TEM image of a Au/Ag core−shell NR (Figure 2b) clearly shows that the Ag shell was homogeneously coated around the Au NR with an average shell thickness of ~4 nm. The shell thickness can be controlled by the amount of Ag deposited on the Au NR seeds. The prepared Au/Ag core−shell NRs are highly monodisperse, and their aspect ratios have a quite narrow Gaussian distribution as shown in Figure 2c. From the synthetic point of view, this method offers a rapid and uniform coating process. Compared to the previously reported complicated methods that require rigorously maintaining a constant pH value and weak reduction environment,[13,22] our method can give homogeneous coating on Au NRs even though a strong reducing agent ($NaBH_4$) was used.

Figure 3a shows the extinction spectra of the Au NRs and Au/Ag core−shell NRs with different Ag shell thickness (2 and 4 nm). Au/Ag core−shell NRs displayed two transverse modes at 400 and 510 nm, which correspond to the contributions of Ag and Au, respectively. However, only one longitudinal SPR band was observed in the bimetallic Au/Ag core−shell NRs. The longitudinal SPR bands of Au/Ag core−shell NRs were found to be very sensitive to the thickness of Ag coating. As the thickness

dx.doi.org/10.1021/jp201648v |J. Phys. Chem. C XXXX, XXX, 000–000

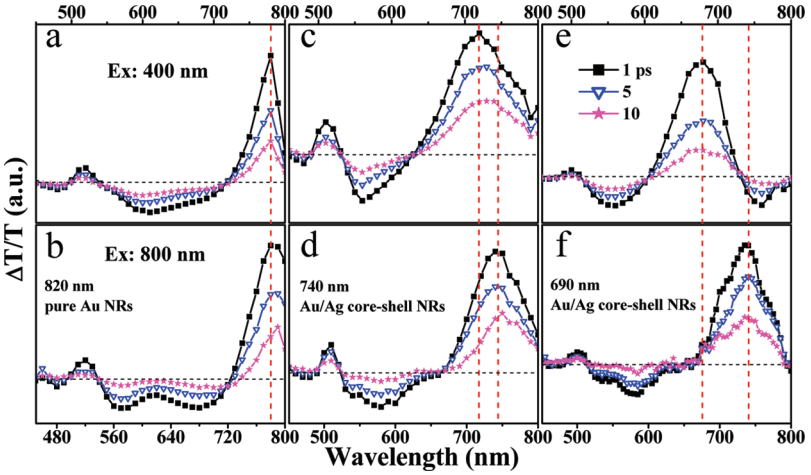

Figure 4. Transient absorption spectra of the original pure Au NRs (a, b) and Au/Ag core−shell NRs with longitudinal SPR at 740 nm (c, d) and 690 nm (e, f), respectively. The upper panels show the transient spectra of different samples under excitation at 400 nm, and the lower panels show the corresponding transient spectra under excitation at 800 nm. The excitation fluences of 400 and 800 nm are both ~50 $\mu J/cm^2$.

of Ag coating increased, the longitudinal SPR gradually shifted to blue. The band maxima could be tuned from 820 to 690 nm. The bandwidth of the Au/Ag core−shell NRs became slightly narrowed (by ~20%) compared to pure Au NRs, which was previously explained as plasmon focusing.[21]

The theoretical extinction spectra of Au/Ag core−shell NRs were simulated by using the DDA model, which has been demonstrated to be a powerful method for calculating the optical spectrum of noble metal nanoparticles.[11,36] The DDA calculations were implemented by employing the freely available DDSCAT 7.0 code developed by Draine and Flatau.[37,38] The nanorod shape was modeled as a cylinder with hemispherical end-caps, which was described by an array of dipoles of a cubic unit with lattice dimension of 0.5 nm. The complex refractive indices of Au and Ag were extracted from the literature.[39] The refractive index of the surrounding aqueous medium was assumed to be 1.33. Figure 3b shows the simulated extinction spectra of Au NRs and Au/Ag core−shell NRs with different amounts of Ag coating. Only one longitudinal SPR band was obtained in the simulated extinction spectra of Au/Ag core−shell NRs, similar to the experimental observations. The longitudinal SPR band gradually shifts to blue and acquires higher intensities as the Ag shell thickness increases, which is in good agreement with the experimental observations.

Ma[18] and Zhu[19] have demonstrated that bimetallic Au/Ag core−shell nanoparticles can support two transverse SPR bands. It is thus reasonable to expect that there are two longitudinal SPR bands in Au/Ag core−shell NRs. However, only one longitudinal SPR band was obtained from the UV−visible extinction spectra and the DDA simulation results. To resolve this conflict and further understand the nature and origin of the SPR bands, we have employed ultrafast transient absorption spectroscopy to study these Au/Ag core−shell NRs. The transient absorption experiments on pure Au NRs and Au/Ag core−shell NRs have been conducted under two different excitation wavelengths: 400 and 800 nm (Figure 4).

Figures 4a and 4b show the transient absorption spectra of pure Au NRs at different delay times under excitation at 400 and 800 nm, respectively. The spectra are quite similar under two different excitation wavelengths: the transient bleaching of both longitudinal and transverse bands was observed with transient absorption in the wings of the band. The longitudinal band bleaching is the dominant feature in the transient absorption spectra. The longitudinal band bleaching is centered at 780 nm for both 400 and 800 nm excitations. In a transient absorption experiment, the conduction band electrons in Au NRs are promoted to an elevated electronic temperature through interband and intraband transitions under excitation at 400 and 800 nm, respectively. Except for the first few tens of femtoseconds, the transient absorption spectra of pure Au NRs will be very similar for intraband and interband excitations.[25,26,28,30,40,41] Therefore, the bleaching peaks of the longitudinal mode in pure Au NRs are very similar under excitation at 400 and 800 nm.

The transient absorption spectra of Au/Ag core−shell NRs are significantly different from those of pure Au NRs. Au/Ag core−shell NRs with a steady state longitudinal SPR band maximum at 740 nm exhibited a transient longitudinal bleaching peak at 720 and 740 nm under excitation at 400 and 800 nm, respectively (Figure 4c and d). The difference in the transient longitudinal bleaching peaks under different excitation wavelengths became even larger for Au/Ag core−shell NRs with a steady state longitudinal SPR band maximum at 690 nm. Their transient longitudinal bleaching peaks were found to center at 680 and 740 nm under excitation at 400 and 800 nm, respectively (Figure 4e and f).

The different results for pure Au NRs and Au/Ag core−shell NRs suggest that the Ag shell also contributes to the observed plasmon resonance. Upon the Ag coating, the longitudinal SPR band of Au NRs will shift to blue due to the change in the surrounding dielectric medium. At the same time, the semicone or rodlike Ag shell has its own longitudinal mode, which is estimated to be centered around 600−700 nm depending on its size.[12] Under excitation at 800 nm, 800 nm laser pulses selectively excite the Au NR core, while the Ag shell will be less excited due to off-resonance. This is particularly more significant for core−shell NRs with a thicker Ag shell, in which the decreased aspect ratio will further shift its longitudinal SPR band to a shorter wavelength. The observed longitudinal SPR bleaching signal under excitation at 800 nm was mainly due to the contribution from the Au core. Although the steady state longitudinal SPR of the Au/Ag core−shell NRs shifts to blue as the Ag shell thickness increases, the dimension of the Au NR core does not change. Therefore, the longitudinal SPR bleaching maximum obtained for different Au/Ag core−shell NRs with

dx.doi.org/10.1021/jp201648v |J. Phys. Chem. C XXXX, XXX, 000–000

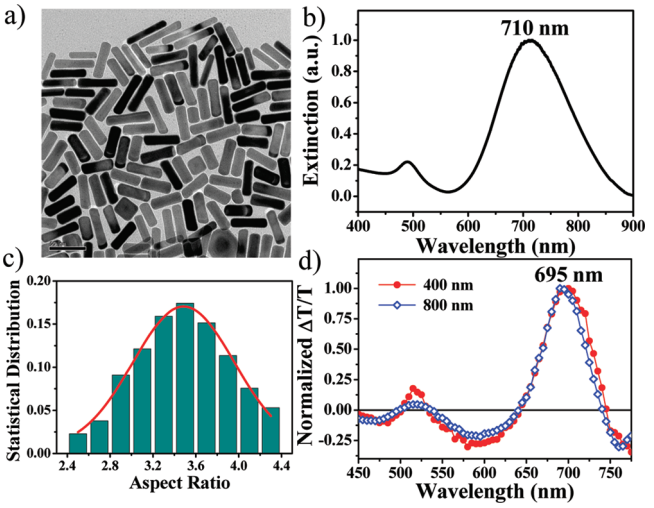

Figure 5. (a) TEM image of pure Au NRs and (b) the corresponding extinction spectrum. (c) Histogram of the aspect ratio distribution of NRs and the corresponding Gaussian fit. The statistical analysis of aspect ratio was evaluated from TEM imaging of more than 200 nanoparticles. (d) Transient absorption spectra of Au NRs at a delay time of 1 ps after excitation at 400 and 800 nm.

different Ag shell thickness nearly does not change under excitation at 800 nm. This explains why both Au/Ag core−shell samples give a longitudinal SPR bleaching maximum at 740 nm (Figure 4d and f), although their steady state longitudinal band maxima are quite different.

The situation is different under excitation at 400 nm. Both the Ag shell and Au core components will be excited via intraband (excitation of the Ag transverse band) or interband transition (for Au)[40] by the 400 nm laser pulses and contribute to the transient absorption/bleaching signals. The overall transient absorption signal of the core−shell NRs is a combination of optical responses of both Ag and Au components. The bleaching of the longitudinal SPR band would thus be expected to be similar to that of steady state SPR spectra. This is consistent with the observation that, under excitation at 400 nm, the longitudinal bleaching peaks are located at 680 and 720 nm for the Au/Ag core−shell NRs with a steady state longitudinal SPR band centered at 690 and 740 nm, respectively.

One possible explanation for the observation of different transient longitudinal SPR bleaching peaks under excitation at 400 and 800 nm is the inhomogeneity in the morphology, size, or aspect ratio of the nanoparticles. The excitation at different wavelengths may selectively excite a particular group of nanoparticles in the inhomogeneous distribution. However, the TEM images of the prepared Au/Ag core−shell NRs show that these samples are of high quality with pretty uniform Ag shell coating (Figure 2a). We have also done control experiments to further exclude the possibility of selective excitation due to sample inhomogeneity. We have conducted similar experiments on pure Au NRs with the steady state longitudinal SPR band centered at 710 nm (Figure 5). This nanorod sample has an even larger distribution of aspect ratio (thus more inhomogeneous). However, the transient longitudinal SPR bleaching bands at 695 nm were observed for excitation wavelength at both 400 and 800 nm. If the selective excitation is due to sample inhomogeneity, it should apply to the pure Au NRs as well; i.e., different longitudinal SPR bleaching bands would be expected under excitation at 400 and 800 nm. This is contradictory to our observations. Similarly, the observation of an even larger difference in the transient longitudinal bleaching peaks for Au/Ag core−shell NRs with a thicker Ag shell (Figure 4) suggests that the selective excitation is because of different contributions of the core−shell NRs due to the change in compositions instead of sample inhomogeneity. The selective excitation is more likely due to two longitudinal SPR contributions arising from the Au core and Ag shell components in the Au/Ag core−shell NRs. The reason that only one longitudinal SPR band is generally seen in UV−visible extinction spectrum is because two longitudinal bands are closely spaced and merge into one band, while two widely spaced transverse SPR bands are distinctly observed due to their larger difference in resonance energies.

These results clearly show that transient absorption spectroscopy provides in-depth insight into understanding the optical characteristics of the probed medium. The different contributions of the Au core and Ag shell of the Au/Ag core−shell NRs can be unambiguously differentiated by selective excitation using different excitation wavelengths, which are otherwise hidden in the broad steady state extinction spectra.

CONCLUSION

In summary, we have developed a facile method to synthesize Au/Ag core−shell NRs. The formation of the uniform Ag shell was confirmed by transmission electron microscopy and UV−visible extinction spectra. The longitudinal SPR band of Au/Ag core−shell NRs can be tuned by controlling the thickness of Ag grown over the Au NR surface. The steady state optical properties of Au/Ag core−shell NRs have also been modeled by DDA simulations. Although these Au/Ag core−shell NRs are expected to display two longitudinal SPR bands, only one longitudinal SPR band was observed in the UV−vis extinction spectra and simulation results. This conflict was resolved by using ultrafast transient absorption spectroscopy under different excitation wavelengths: 400 and 800 nm. We have experimentally demonstrated for the first time the existence of two longitudinal SPRs in Au/Ag core−shell NRs, arising from the Ag shell and Au core. Only one longitudinal SPR band is generally seen in the steady state UV−vis extinction spectrum because two closely spaced longitudinal SPR bands merge into one band. Transient absorption spectroscopic studies help to provide a more in-depth understanding of the nature of the optical characteristics of these metal nanomaterials, which are otherwise hidden in the broad steady state optical spectra.

AUTHOR INFORMATION

Corresponding Author

*E-mail: chmxqh@nus.edu.sg.

ACKNOWLEDGMENT

This work is supported by the Faculty of Science, National University of Singapore (R-143-000-341-112). We thank Prof. Bruno Palpant (CNRS) for helpful discussions and Mr. Yih Hong Lee for the help in reading through the manuscripts.

REFERENCES

(1) Anker, J. N.; Hall, W. P.; Lyandres, O.; Shah, N. C.; Zhao, J.; Van Duyne, R. P. *Nat. Mater.* **2008**, *7*, 442.

(2) Yu, C. X.; Irudayaraj, J. *Anal. Chem.* **2007**, *79*, 572.
(3) Wang, C. G.; Chen, Y.; Wang, T. T.; Ma, Z. F.; Su, Z. M. *Adv. Funct. Mater.* **2008**, *18*, 355.
(4) Murphy, C. J.; Gole, A. M.; Hunyadi, S. E.; Stone, J. W.; Sisco, P. N.; Alkilany, A.; Kinard, B. E.; Hankins, P. *Chem. Commun.* **2008**, *5*, 544.
(5) Wang, H. F.; Huff, T. B.; Zweifel, D. A.; He, W.; Low, P. S.; Wei, A.; Cheng, J. X. *Proc. Natl. Acad. Sci. U.S.A.* **2005**, *102*, 15752.
(6) Durr, N. J.; Larson, T.; Smith, D. K.; Korgel, B. A.; Sokolov, K.; Ben-Yakar, A. *Nano Lett.* **2007**, *7*, 941.
(7) Zhao, T. T.; Wu, H.; Yao, S. Q.; Xu, Q. H.; Xu, G. Q. *Langmuir* **2010**, *26*, 14937.
(8) Huang, X. H.; El-Sayed, I. H.; Qian, W.; El-Sayed, M. A. *Nano Lett.* **2007**, *7*, 1591.
(9) Zijlstra, P.; Chon, J. W. M.; Gu, M. *Nature* **2009**, *459*, 410.
(10) Chon, J. W. M.; Bullen, C.; Zijlstra, P.; Gu, M. *Adv. Funct. Mater.* **2007**, *17*, 875.
(11) Kelly, K. L.; Coronado, E.; Zhao, L. L.; Schatz, G. C. *J. Phys. Chem. B* **2003**, *107*, 668.
(12) Sanchez-Iglesias, A.; Carbo-Argibay, E.; Glaria, A.; Rodriguez-Gonzalez, B.; Perez-Juste, J.; Pastoriza-Santos, I.; Liz-Marzan, L. M. *Chem.—Eur. J.* **2010**, *16*, 5558.
(13) Xiang, Y. U.; Wu, X. C.; Liu, D. F.; Li, Z. Y.; Chu, W. G.; Feng, L. L.; Zhang, K.; Zhou, W. Y.; Xie, S. S. *Langmuir* **2008**, *24*, 3465.
(14) Duan, J. S.; Park, K.; MacCuspie, R. I.; Vaia, R. A.; Pachter, R. *J. Phys. Chem. C* **2009**, *113*, 15524.
(15) Purcell, E. M.; Pennypac, Cr *Astrophys. J.* **1973**, *186*, 705.
(16) Cardinal, M. F.; Rodriguez-Gonzalez, B.; Alvarez-Puebla, R. A.; Perez-Juste, J.; Liz-Marzan, L. M. *J. Phys. Chem. C* **2010**, *114*, 10417.
(17) Hao, F.; Nehl, C. L.; Hafner, J. H.; Nordlander, P. *Nano Lett.* **2007**, *7*, 729.
(18) Ma, Y. Y.; Li, W. Y.; Cho, E. C.; Li, Z. Y.; Yu, T. K.; Zeng, J.; Xie, Z. X.; Xia, Y. N. *ACS Nano* **2010**, *4*, 6725.
(19) Zhu, J. *Nanoscale Res. Lett.* **2009**, *4*, 977.
(20) Liu, M. Z.; Guyot-Sionnest, P. *J. Phys. Chem. B* **2004**, *108*, 5882.
(21) Becker, J.; Zins, I.; Jakab, A.; Khalavka, Y.; Schubert, O.; Sonnichsen, C. *Nano Lett.* **2008**, *8*, 1719.
(22) Okuno, Y.; Nishioka, K.; Kiya, A.; Nakashima, N.; Ishibashi, A.; Niidome, Y. *Nanoscale* **2010**, *2*, 1489.
(23) Logunov, S. L.; Ahmadi, T. S.; El-Sayed, M. A.; Khoury, J. T.; Whetten, R. L. *J. Phys. Chem. B* **1997**, *101*, 3713.
(24) Guillet, Y.; Charron, E.; Palpant, B. *Phys. Rev. B* **2009**, *79*, 195432.
(25) Jiang, Y.; Wang, H. Y.; Xie, L. P.; Gao, I. R.; Wang, L.; Zhang, X. L.; Chen, Q. D.; Yang, H.; Song, H. W.; Sun, H. B. *J. Phys. Chem. C* **2010**, *114*, 2913.
(26) Link, S.; Burda, C.; Mohamed, M. B.; Nikoobakht, B.; El-Sayed, M. A. *Phys. Rev. B* **2000**, *61*, 6086.
(27) Link, S.; El-Sayed, M. A. *J. Phys. Chem. B* **1999**, *103*, 8410.
(28) Bigot, J. Y.; Halte, V.; Merle, J. C.; Daunois, A. *Chem. Phys.* **2000**, *251*, 181.
(29) Voisin, C.; Del Fatti, N.; Christofilos, D.; Vallee, F. *J. Phys. Chem. B* **2001**, *105*, 2264.
(30) Hartland, G. V. *Annu. Rev. Phys. Chem.* **2006**, *57*, 403.
(31) Nikoobakht, B.; El-Sayed, M. A. *Chem. Mater.* **2003**, *15*, 1957.
(32) Busbee, B. D.; Obare, S. O.; Murphy, C. J. *Adv. Mater.* **2003**, *15*, 414.
(33) Thierry, B.; Ng, J.; Krieg, T.; Griesser, H. J. *Chem. Commun.* **2009**, *13*, 1724.
(34) Leonov, A. P.; Zheng, J. W.; Clogston, J. D.; Stern, S. T.; Patri, A. K.; Wei, A. *ACS Nano* **2008**, *2*, 2481.
(35) Henglein, A.; Giersig, M. *J. Phys. Chem. B* **1999**, *103*, 9533.
(36) Myroshnychenko, V.; Rodriguez-Fernandez, J.; Pastoriza-Santos, I.; Funston, A. M.; Novo, C.; Mulvaney, P.; Liz-Marzan, L. M.; de Abajo, F. J. G. *Chem. Soc. Rev.* **2008**, *37*, 1792.
(37) Draine, B. T.; Flatau, P. J. *J. Opt. Soc. Am. A* **1994**, *11*, 1491.
(38) Draine, B. T. Flatau, P. J. http://arXiv.org/abs/1002.1505v1 (accessed 2010).
(39) Johnson, P. B.; Christy, R. W. *Phys. Rev. B* **1972**, *6*, 4370.
(40) Yu, K.; Polavarapu, L.; Xu, Q. H. *J. Phys. Chem. A* **2011**, *115*, 3820.
(41) Del Fatti, N.; Voisin, C.; Achermann, M.; Tzortzakis, S.; Christofilos, D.; Vallee, F. *Phys. Rev. B* **2000**, *61*, 16956.